Optimization of construction safety inspection path from the perspective of risk

Naiwen Li[a], Qibin Yuan[b*], Jian Dai[c]

School of Business and Management, Liaoning Technical University, Huludao 125105, China;

[a]2013227081@qq.com, [b*]790935304@qq.com, [c]yqb123321@163.com

Abstract: Safety inspection work often determines the probability of accidents in construction, but also affects the production cost of work, to improve the quality and efficiency of construction safety inspection work, it is very important to propose a patrol inspection strategy.By comprehensively considering risk factors, a safety inspection path is formed. The objective function is constructed the RP-ACO (Risk Probability-ACO) algorithm is proposed, and based on the original ACO algorithm, the segmentation function is introduced to adjust the pheromone strength by changing the state transition rule Simulation results show that when only the risk probability value is considered, the average objective function of the RP-ACO algorithm is 20.0573, and the average number of convergences is 110.6 times, which has great advantages over the 20.0639 and 232.2 In the oliver30 test case, the minimum value of the RP-ACO algorithm is 423.9117, and the average value is 425.8249, which has obvious advantages over the original ACO algorithm, It can be seen that with the increase of emission reduction measures and the increase of spacing, the superiority of the RP-ACO algorithm is more than that of the original ACO algorithm, which has obvious advantages over the original ACO of 425.8201 and 429.0233. It can be seen that with the increase of emission reduction measures and the increase of spacing, the superiority of the RP-ACO algorithm is more obvious. Taking the safety inspection work of a construction site as an example, the inspection workload and inspection time under different paths were analyzed, and the correctness and effectiveness of the proposed safety inspection The results show that the inspection path formulated according to the construction safety risk can The results show that the inspection path formulated according to the construction safety risk can effectively reduce the inspection workload. At the same time, the inspection path optimization algorithm designed by the RP-ACO algorithm is used. At the same time, the inspection path optimization algorithm designed by the RP-ACO algorithm is used to realize the optimization of inspection.

Key words: Safety patrol; Risk probability value; Path optimization; RP-ACO algorithm; Risk perspective

1. Introduction

On construction sites, safety inspections are especially important as they are loaded with the safety of workers and production costs. In the previous inspection process, safety officers often decided the inspection order according to their preferences. Nowadays, with the development of intelligent construction sites, inspection efficiency will be improved by introducing intelligence into the preparation of inspection paths. The construction site in the regional conditions are different, and its risk probability value is also different if combined with the risk

EMIS 2023, February 24-26, Chengdu, People's Republic of China

DOI 10.4108/eai.24-2-2023.2330649

probability value for inspection.

In the problem of path optimization, algorithms such as Guo[1] 2021 adopted swarm, Bai[7] 2021 adopted simulated annealing, Zhu[16] 2020 adopted neural network, Wang[13] 2020 adopted genetic and 2021Chen[2] adopted A* are widely used. However, these algorithms also have some drawbacks, such as poor robustness, local miniaturization, and insufficient adaptability. Colorni[3] 1991,2000 Dorigo[4] Dorigo[5] 2002,Khaled[10] 2018 , Ye[16] 2020 put forward The robustness of the ant colony algorithm has some advantages over other algorithms, with the features of positive feedback, high robustness and parallelism, and strong intelligent search capability, so the ant colony algorithm is the preferred to solve the path optimization problem. However, the ant colony algorithm also has defects, and it is easy to fall into the dilemma of local optimum and slow convergence speed. In this paper, we make improvements to the traditional ant colony algorithm according to He[8] 2021, Zhang[17] 2017, Ma[12] 2021, Liu[11] 2004, which improves the convergence speed and the optimal searchability of the ant colony.

For the construction site safety inspection path optimization problem, firstly, the scoring method is used to construct a risk probability model for each area of construction, Secondly, the risk probability model is combined with the path shortest model, again the traditional ant colony algorithm is improved, and finally. 20 areas of a construction site are used as a model for simulation to confirm the feasibility of the study.

2. Problem description and model

The safety inspection problem is similar to the TSP problem, where the safety officer does not repeat the point inspection of the equipment during the inspection. Specific description: A safety officer, with a set of areas *N*, starts from the first area and inspects the remaining areas of N-1 until the inspection is completed. Correspondingly and at the same time to meet the constraints: the safety officer can only be inspected within the scope of the site, that is, within the specified scope, and only once for each area.

The safety officer can check the area based on the path length and the magnitude of the risk probability value. The first two optimization objectives are to determine the path length optimization and the risk probability value.

① Optimal path:

$$\min f_1 = \sum_{i=1,\ j=1}^{N} L_{i,j} \tag{1}$$

② The probabilistic model of risk probability is specified as follows.

$$\min f_2 = \sum_{i=1,\ j=1}^{N} PR_j / PR_i \tag{2}$$

In Eq. 2: i, j are regions.

(iii) The above two objectives are dimensionless by normalization, and the function F_{ij} is formed by adding the weight coefficients ω1 and ω2.

$$F_{ij} = \omega_1 \sum_{i=1,\ j=1}^{N} L_{i,j} + \omega_2 \sum_{i=1,j=1}^{N} PR_j / PR_i \tag{3}$$

In equation (3): $F_{i,j}$ is the objective function; N is the number of inspection regions, $L_{i,j}$ is the distance between 2 regions i,j in the inspection process, PR_i, PR_j refers to the risk probability value of region i, region *j respectively*; ω1 and ω2 are the weighting coefficients, if the priority path is the shortest, then increase the value of ω1; if the priority risk probability value is large, then increase the value of ω2.

Constraints in the mathematical model.

1) $X_{i,j}$ is 1 means the inspector walks from area i to area j, otherwise, it is 0.

2) Only one inspection per region.

$$\sum_{j \in N \cup S,\ j \neq i} \sum x_{ij} = 1, i \in N \tag{4}$$

$$\sum_{i \in N \cup S,\ i \neq j} \sum x_{ij} = 1, j \in N \tag{5}$$

3) The safety officer will look for the next area after completing the inspection of one area.

$$\sum_{i \in N, i \neq j} x_{ih} = \sum_{j \in N, j \neq h} x_{hj}, h \in N \tag{6}$$

3. Site risk probability value model

3.1 Construction site safety risk classification.

1) Weather factor: The weather conditions on the day of inspection by the safety officer are different. 2) Equipment factor: The equipment used is different. 3) Personnel factor: The ability of construction personnel to pay attention to safety is different. 4) Environmental factor: The environment in which the construction is carried out is different. 5) Management factor: The system of the company regarding safety.

In summary, Wang[14] 2020, Fang[6] 2020 the probability of construction safety risks is mainly influenced by environmental, equipment, management, weather, and human factors.

3.2 Site construction safety risk probability model

In classifying the site construction safety risks, the above influencing factors are represented by D1-D5. The values in the initial decision table are the scores (scores are integers of (0, 10]) scored by the project team according to the actual situation in each area.

For the weight assignment of D1-D5, industry experts discussed and finally determined the weights of D1-D5 as 10%, 20%, 30%, 30%, and 10%, respectively. The mathematical expression of the probability of construction safety risk is

$$D = 0.1 * D1 + 0.2 * D2 + 0.3 * D3 + 0.3 * D4 + 0.1 * D5 \tag{7}$$

$$P_f = D / 10 \tag{8}$$

In equation (8): *D is the* total score and P_f is the risk probability.

Table 1 Initial Decision Table

D1	D2	D3	D4	D5
8	9	9	9	8
7	8	6	7	5
...	...	...	...	...
8	9	6	6	4

In Table 1: D1 is the weather factor; D2 is the equipment factor; D3 is the personnel factor; D4 is the environmental factor; and D5 is the management factor.

4. RP-ACO algorithm

For the inspection path optimization problem considering the probability value of security risk, the optimization method of the improved ant colony is selected. The improvement points are mainly divided into two aspects: one is to improve the state transfer rule to increase the randomness of the search path; the second is to introduce the segmentation function to adjust the pheromone intensity to achieve the optimization of the point inspection path.

4.1 Improvements to the transfer probability

The traditional transfer idea of ant the long algorithm is to first determine all feasible points in the next step and then select a point from the feasible points as the next path point by the roulette principle according to the calculated transfer probability Zhu[9] 2021. The mathematical expression for the transfer probability of feasible points is

$$P_{ij}^{k} = \begin{cases} \dfrac{\tau_{ij}(t)^{\alpha} . \eta_{ij}(t)^{\beta}}{\sum_{s \in allow_k} \tau_{\text{ij}}(t)^{\alpha} . \eta_{ij}(t)^{\beta}} & \text{j} \in allow_k \\ 0 & \end{cases} \tag{9}$$

In equation (9): P_{ij} k denotes the probability of ant *k* moving from *I* to *j;* τ_{ij} (t) denotes the pheromone concentration from *I* to *j*, η_{ij} (t) denotes the inverse of the distance between two path points *I,j* i.e. $1/d_{\text{ij}}$, also denotes the visibility of ants from *I* to *j*; *allow* is the set of nodes that have not been visited yet, *α is the* pheromone factor, which takes values usually between [1,4]; *β* is the heuristic function factor, which takes values range is usually between [0,5].

The roulette wheel path selection method has a small probability of selecting the optimal path when the weighted product of pheromones and heuristic information is not large. The pseudo-random distribution transfer rule makes the ant colony more inclined to choose the path with more pheromones and thus the optimal path. The specific expressions are as follows.

$$P_j = \begin{cases} \underset{s \in allow_k}{\arg\max} \left\{ [\tau_{is}(t)]^{\alpha} [\eta_{is}(t)]^{\beta} \right\}, & q < q_0 \\ P_{ij}^k \end{cases} \tag{10}$$

In equation (10): q is a random number uniformly distributed in the interval [0,1], which is used to regulate the random search ability of the algorithm for new paths, such that $q_0 = 0.1$. When the point inspector selects the device, a random number q is first generated, and later the transfer method is determined by comparing the magnitude of q and q_0

4.2 Adjustment of pheromone intensity Q

Pheromones are divided into global updates and local updates.

① Pheromone global update expressions.

$$\tau_{ij}(t+1) = \tau_{ij}(t) \times (1-\rho) + \Delta\tau_{ij}, 0 < \rho < 1; \Delta\tau_{ij} = \sum_{k=1}^{m} \Delta\tau_{ij}^k \tag{11}$$

$$\Delta\tau_{ij}^k = \begin{cases} \frac{Q}{F_K}, \mathit{If\ ant\ K\ passes\ the\ pathpoint\ i\ to\ j} \\ 0,\ or \end{cases} \tag{12}$$

② Pheromone local update expressions:

$$\tau_{ij}(t+1) = \tau_{ij}(t) \times (1-\rho) \tag{13}$$

In Eqs. (11-13): τ_{ij} (t+1) denotes the pheromone concentration on the device *i* to *j* at t+1 cycles; ρ denotes the pheromone volatility factor; $\Delta\tau_{ij}$ denotes the pheromone increment of ant *k* through device *i* to *j*; *Q* is a constant; and F_k denotes the path of ant *k. The* ability of the ant colony algorithm to search for paths can be changed by varying Δτij in the global update formula of pheromone.

To enable the ant colony to choose the optimal path effectively when the pheromone on the path changes, the pheromone constant *Q is* transformed into a segmentation function Q_t, and different values are taken at different iterations. The pheromone can be set to a smaller value at the early stage of ant colony action, which is used to enhance the searchability of the algorithm; in the middle stage, it is necessary to speed up the search speed of the algorithm for new paths and avoid the pheromone being too small to fall into a chaotic state, so the *Q* value should be set larger in the middle stage. At the later stage, the optimal path has been found, so the *Q value is set* to the maximum, to converge to the optimal path quickly. The mathematical expression of the pheromone segmentation function is

$$Q_t = \begin{cases} 8, 1 \le t < 0.3t_{max} \\ 10, 0.3t_{max} \le t \le 0.6t_{max} \\ 14, 0.6t_{max} < t \le t_{max} \end{cases} \tag{14}$$

4.3 Parameter setting

The setting of parameters affects the performance of the ant colony algorithm to some extent, so reasonable parameters need to be set. The values of two parameters are set as quantitative, and the test is performed by changing another variable. The initial default parameters were set as α=1, β=1, ρ=0.1, m=70, the number of iterations was 200, and the determination was performed on the probability of risk value model (ω1=0, ω2=1) with ten determinations.

The values of ①ρ are shown in Table 2.

Table 2 Value of ρ

ρ	0.1	0.2	0.3	0.4	0.5	0.6	0.7	0.8	0.9
Max	20.1406	20.1249	20.132	20.1231	20.1307	20.1256	20.13	20.1247	20.1433
Avg	20.1126	20.1085	20.1080	20.1080	20.115	20.113	20.1078	20.1127	20.1140
Min	20.0879	20.0815	20.0838	20.0925	20.0984	20.1073	20.0756	20.0951	20.0914

From the data in Table 2, it can be seen that when ρ = 0.7, its three worthy data are better than other values.

② The values of the number of iterations (α=1, β=1, ρ=0.7) are shown in Table 3.

Table 3 Value of t

t	100	200	300
Max	20.1434	20.13	20.1266
Avg	20.1252	20.1078	20.1013
Min	20.1009	20.0756	20.0758

From the data in Table 3, it can be seen that when the number of iterations is 300, its objective function value is at a clear advantage.

③ The values of α (β=1,ρ=0.7,t=300) were taken as shown in Table 4.

Table 4 Value of α

α	1	2	3
Max	20.1266	20.2399	20.2528
Avg	20.1013	20.1821	20.2138
Min	20.0758	20.1504	20.1751

From the data in Table 4, it is clear that when α = 1, its objective function value is a clear advantage.

④ The values of β (α = 1, ρ = 0.7, t = 300) are shown in Table 5.

Table 5 Value of β

β	1	2	3	4
Max	20.1266	20.0928	20.0852	20.0654
Avg	20.1013	20.0845	20.0711	20.0589
Min	20.0758	20.0703	20.0564	20.0522

From the data in Table 5, it is clear that when β = 4, its objective function value is a clear advantage.

In summary, the final parameters are set as α=1, β=4, ρ=0.7, m=70, and the number of iterations is 300.

4.4 Improved algorithm flow

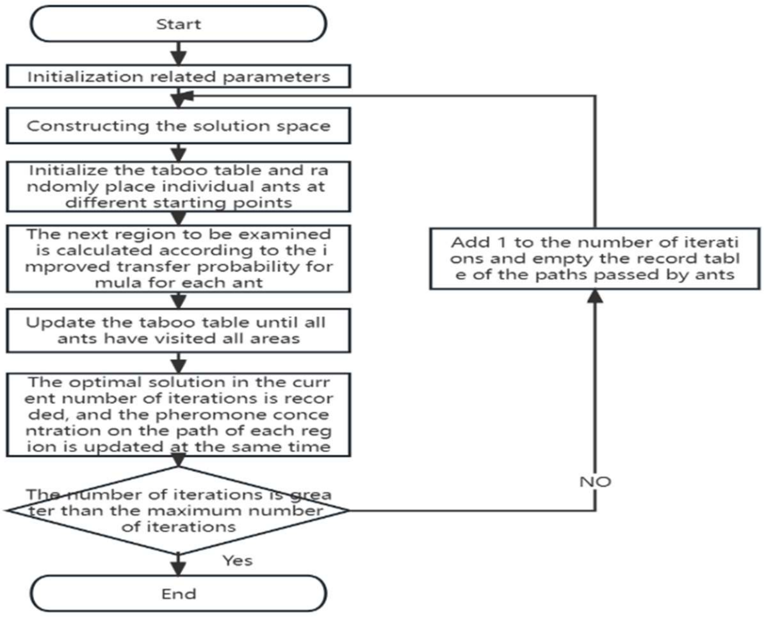

4.5 Algorithm Time Complexity Analysis

Zhu[9] 2021 Algorithm complexity analysis of RP-ACO: It is known that *N* is the number of devices, *m* is the number of ants, and *T* is the number of iterations. In each iteration, the complex consists of the complexity of population initialization O(m*N), the complexity of generating ant paths using transfer probability rules O(m*N^2), the complexity of recording the optimal paths of m ant iterations O(m*(N-1)), and the complexity of updating the pheromone values O(m*(N-1)) as O(m*N $)^2$.

Thus the complexity of the RP-ACO algorithm is TRP-ACO = O(T*(m*N^2)).

5. Experimental case study

5.1 Experimental cases

In this case, a construction site is selected as a sample for a safety inspection, and Figure 1 shows the manual inspection roadmap. Table 6 shows the coordinate values and risk probability values of the area facilities.

Table 6 Motor coordinate value and its risk probability value

X	1	1	1	1	3	3	3	3	5	5
Y	10	8	5	3	9	7	4	2	10	9
Risk probability value	0.88	0.68	0.85	0.56	0.84	0.63	0.92	0.63	0.65	0.78
X	5	5	5	5	6	6	7	7	8	8
Y	8	5	4	3	7	6	7	6	7	6
Risk probability value	0.89	0.68	0.76	0.96	0.76	0.94	0.82	0.85	0.71	0.66

5.2 Selection of weights

The respective optimal paths are selected for weights ω1=1, ω2=0; ω1=0,ω2=1.

①When ω1=1,ω2=0, i.e., when only the shortest path is considered.

The shortest distance of the route is 31.8372; the route through the line is

13→14→8→7→4→3→6→2→1→5 →9→10→11→15→17→9→20→18 →16→12.

② When ω1=0,ω2=1, i.e., when only the probability of risk value is considered.

The shortest distance of the path is 20.0463; the path line is

9→19→15→3→5→11→7→14→16 →1→18→17→10→13→2→12→20 →6→8→4.

Table 7 Comparison of ACO and RP-ACO algorithms

Algorithm / Weights Coefficient		ACO				RP-ACO			
ω1	ω2	Minimum value	Average value	Maximum value	The average number of convergence	Minimum value	Average value	Maximum value	The average number of convergence
0	1	20.0579	20.0639	20.0732	232.3	20.0463	20.0573	20.0654	110.6
1	0	31.8372	31.8372	31.8372	4	31.8372	31.8372	31.8372	3.8

From the data in Table 7, it can be concluded that by comparing the results of the two algorithms run ten times longitudinally and horizontally as well as analyzing them in many aspects, RP-ACO has better values and convergence speed than the traditional algorithm when only the risk probability value is considered; the optimal value of both algorithms is 31.8372 when only the distance is considered, due to the limitation of the process flow and production layout in practice, so the equipment between The distance is close and the number is limited, which leads to a small difference between the two algorithms in this respect.

To further verify the superiority of the RP-ACO algorithm, oliver30 was selected as a test case from TSPLIB and compared with PSO, GA, and ACO algorithms for 20 TSP problem experiments, and the results are shown in Table 8.

Table 8 Comparison table of each algorithm on the TSP problem

Algorithm	Minimum value	Average value	Maximum value
PSO	471.671	525.6646	569.6497
GA	424.9003	460.51573	541.1829
ACO	425.8201	429.0233	432.9609
RP-ACO	423.9117	425.8249	427.1752

From the experimental results in Table 8, it is clear that the RP-ACO algorithm holds a clear advantage.

5.3 Setting of ω1, ω2 weighting coefficients

The problem to be solved is an inspection path optimization problem considering the risk probability value, so both weights must be considered. From the above two sets of data, it can be concluded that the optimization result obtained by considering only the distance is 1.59 times of the optimization result by considering only the risk probability value, which also means that the influence of the distance factor on the objective function is 1.59 times of the risk factor, so the weight ω2 is 1.59 times of the weight ω1, that is, ω1=0.38,ω2=0.62.

When ω1=0.38,ω2=0.62, the shortest route and shortest distance are shown in Figure 1:7→14→13→12→16→18→20 →19→17→15→11→10→9→5→1→ 2→6→3→4→8

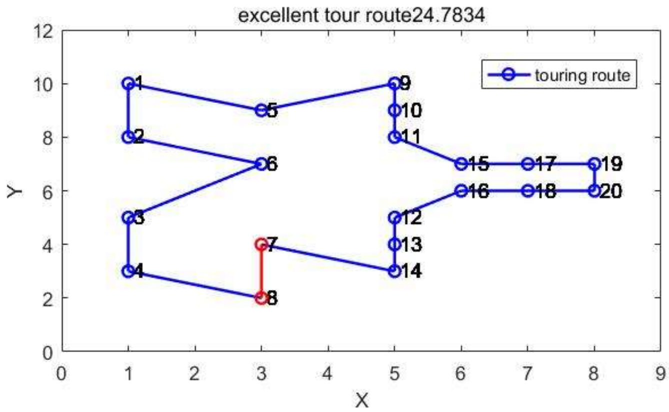

Fig.1 Optimal path graph at ω 1=0.38, ω 2 = 0.62

In the figure: the horizontal axis is the x-axis coordinate of the device, and the vertical axis is the y-axis coordinate of the device. From Figure 2, the shortest distance is 25.1927 (in hundred meters), the blue line is the walking path, and the red line is the connection line between the starting point and the endpoint.

However, it can be found from Figure 1 that it is a complete Hamiltonian circle diagram, and it is obvious that the consideration of the probability of risk values is not thorough enough, so the weight coefficients of both need to be adjusted.

5.4 Adjustment of ω 1, ω 2 weighting coefficients

It is clear from Figures 2 and 3 that when ω1 = 0.06, the path diagram is no longer a clear Hamiltonian circle diagram, but is influenced by the probability-at-risk value, resulting in a change in the path.

And when ω1=0.07, its path diagram begins to gradually approach the Hamiltonian circle, which can also be seen that its consideration of the weight of the path distance dominates the position. Therefore, with ω1=0.06 and ω1=0 as two bounds, the compromise position is taken. That is, the weighting coefficient ω1 is set to 0.03, and ω2 is set to 0.97. Its path diagram is shown in Figure 4. The specific path lines are:12→13→14→7→3→1→5→11→16 →18→17→19→20→15→10→9→6 →2→4→8. Compared to ω1=1, the path line changes considerably when ω2=0. This also indicates that the risk probability value of the equipment has been taken into account in the path planning of the inspection through this adjustment of the weighting factor.

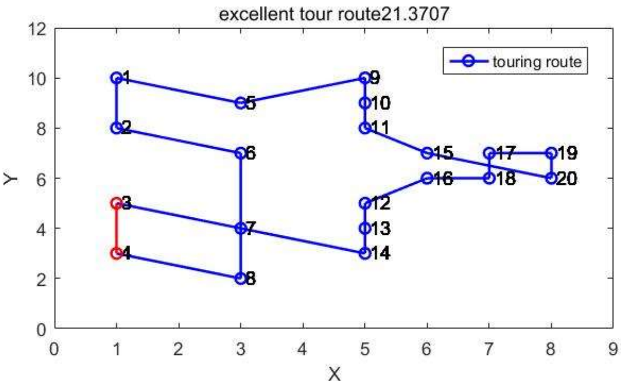

Fig.2 ω 1=0.07, ω 2 = 0.93

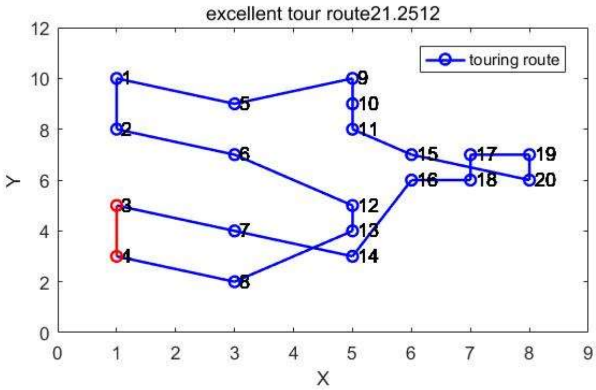

Fig.3 ω 1 = 0.06, ω 2 = 0.94

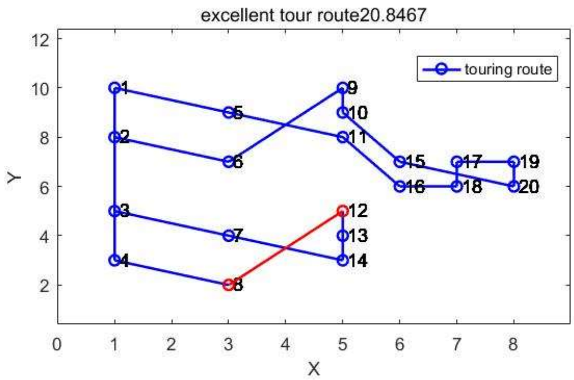

Fig.4 ω 1 = 0.03, ω 2 = 0.97

5.5 Inspection path optimization verification

The path diagram prepared using the algorithm is compared with a manual drawing to illustrate the feasibility of its optimization.

1) Manual experience to determine the inspection path

The inspection route previously used at the site was based on the habits of the safety officer, with a path of [1-2-3-4-5-6-7--20], a distance of 4550m, and a time of about 2 h.

2）Inspection path with the shortest path as the goal

When only the shortest path is considered, the planned path is [13→14→8→7→4→3→6→2 → 1→5→9→10→11→15→17→9→20 →18→16→12.], the distance is 3183 m, and the time taken is about 1.4 h.

3) Consider both path shortest and risk probability

After adjusting the weights for it, this shortest path is [12→13→14→7→3→1→5→11 →16 →18→17→19→20→15→10→9 →6→2→4→8], a distance of 2084 m, and a time of about 1.1 h.

The comparison of different inspection paths is shown in Table 9, and the results show that the inspection efficiency is significantly improved.

Table 9 Comparison of different inspection paths

Strategies	Total inspection distance/m	Total time consumption/h
1	4550	2
2	3183	1.4
3	2084	1.1

6. Conclusion

The improved ant colony algorithm RP-ACO is used to plan the inspection path based on the risk probability value, and the global search capability of the algorithm is enhanced by changing the state transfer rules and introducing segmentation functions to change the pheromone constants.

(1) The inspection path optimization algorithm generated by the RP-ACO algorithm was adopted to achieve the optimization of the inspection path by combining it with the risk probability.

(2) The safety inspection path optimization algorithm based on risk probability values can provide a useful reference for practical work.

(3) The optimization method proposed in this paper improves the efficiency of site safety inspection by human influence, uneven inspection quality, and low efficiency in site safety inspection, and provides a reference for site intelligence.

References

[1] Bai Qin-Yang, Yin Xiao-Qing, Lin Yun. Cold chain logistics path optimization considering real-time traffic in road networks[J]. Industrial Engineering and Management,2021,26(06):56-65.DOI:10.19495/j.cnki.1007-5429.2021.06.007.
[2] Chen Tengfei, Deng Zhongliang, Zhang Zhaohui. Path planning for mobile robots based on improved A~* algorithm[A]. Academic Exchange Center of China Satellite Navigation System Management Office. Proceedings of the 12th Annual China Satellite Navigation Conference - S09 User Terminal Technology[C]. Academic Exchange Center of China Satellite Navigation System Management Office: Organizing Committee of China Satellite Navigation Annual Conference,2021:7.
[3]Colorni A, Dorigo M, Maniezzo V . Distributed Optimization by Ant Colonies[C]// Proceedings of ECAL91 - European Conference on Artificial Life. 1991.
[4]Dorigo M, Bonabeau E, Theraulaz G.Ant algorithms and stigmergy[J].Future Generation Computer Systems, 2000, 16(8):851-871.
[5]Dorigo M, Maniezzo V, Colorni A . Ant system: optimization by a colony of cooperating agents[J]. IEEE Transactions on Systems, Man, and Cybernetics, Part B (Cybernetics), 2002, 26(1):29-41.
[6] Fang J, Hu J, Wei H, Chen ZF, Chen T. Identification of key factors of fall from height human-caused safety risks at construction sites[J]. Journal of Wuhan University of Technology (Information and Management Engineering Edition),2020,42(05):409-413.
[7] Guo Xinghai, Ji Mingjun, Wen Dusu, Zhang Xin, Tian Shuang. Distributed multi-UAV task assignment and path planning for "last-mile" delivery[J]. Systems Engineering Theory and Practice,2021,41(04):946-961.
[8] He ZM, Zheng L, Liang W. Vehicle path planning based on adaptive dynamic search ant colony algorithm[J]. Computer Engineering and Design,2021,42(02):543-551.
[9] JIAYING Zhu, MAO-TING Gao. AUV path planning algorithm incorporating particle swarm and improved ant colony algorithms[J]. Computer Engineering and Applications,2021,57(06):267-273.
[10] Khaled A, Farid K . Mobile robot path planning using an improved ant colony optimization[J]. International Journal of Advanced Robotic Systems, 2018, 15(3):172988141877467-.
[11] Liu S-X, Song J-H, Tang G-F. Ant colony optimization--a review of models, algorithms, and applications[J]. Journal of Systems Engineering,2004(05):496-502.
[12] Ma S.L., Mei H. Global path planning for mobile robots based on improved potential field ant colony algorithm[J]. Journal of Mechanical Engineering,2021,57(01):19-27.
[13] Wang Huaijiang, Liu Xiaoping, Wang Gang, Han Song. Mobile robotic arm picking path optimization based on improved genetic algorithm[J]. Journal of Beijing University of Posts and Telecommunications,2020,43(05):34-40.
[14] Wang Xiaoliang. Research on the influencing factors and control initiatives for the generation of unsafe state of construction site objects [J]. Sichuan Cement,2020(12):333-334.
[15] Ye X, Luo L, Hou L, et al. Laser Ablation Manipulator Coverage Path Planning Method Based on an Improved Ant Colony Algorithm [J]. Applied Sciences, 2020, 10(23):8641.
[16] Zhu DQ, Zhu TT, Yan MZ. Multi-AUV full-coverage path planning based on improved neural networks[J]. Journal of System Simulation,2020,32(08):1505-1514.
[17] Zhang Yu-Xian, Ding Xiu-Kun, Xue Dian-Chun, Wang Xiao-Ting, Cheng Shu-Rui. Scheduling optimization of ant colony algorithm based on memory curve model in flexible job shop[J]. Modern Manufacturing Engineering,2017(11):105-109.DOI:10.16731/j.cnki.1671-3133.2017.11.019.